

# Reinvestigation and Structural Approach of the Ba–Pt–O System for $\frac{4}{3} < Y = \text{Ba/Pt} < \frac{5}{2}$

F. Grasset, F. Weill, and J. Darriet

*Institut de Chimie de la Matière Condensée de Bordeaux, CNRS-UPR 9048, Avenue du Docteur Albert Schweitzer, 33608 Pessac Cedex, France*

Received July 8, 1997; in revised form November 20, 1997; accepted January 26, 1998

A reinvestigation of the Ba-rich region of the Ba–Pt–O system has been undertaken. The existence of a solid solution, already mentioned, has been confirmed, and its true formulation has been determined:  $\text{Ba}_{12}[\text{Ba}_x\text{Pt}_{3-x}]\text{Pt}_6\text{O}_{27}$  with  $0 \leq x \leq 3$ . The structure of these phases can be schematically considered as being built up from the periodic stacking along the *c* direction of one close-packing  $[\text{Ba}_3\text{O}_9]$  layer, similar to those of the hexagonal perovskite, and three  $[\text{Ba}_3A'\text{O}_6]$  layers, with  $A' = \text{Ba, Pt}$ . The stacking of these mixed layers is of hexagonal type, and then columns parallel to *c* are formed. They consist of octahedra and trigonal prisms, sharing faces, which are occupied by  $A'$  cations. For  $0 \leq x \leq 1$ , the structure appears to be incommensurate and should be described as a composite crystal based on two subsystems:  $[\text{Ba}]$  and  $[(\text{Ba, Pt})\text{O}_3]$ . For  $x > 1$ , the X-ray diffraction pattern can be explained using a three-dimensional cell, but the structure refinement attempts as well as the electron diffraction patterns seem to indicate these phases are commensurate modulated structures. © 1998 Academic Press

## INTRODUCTION

Recently the chemistry of platinum ternary and quaternary oxides has undergone considerable progress. This interest is mainly due to the potential use of their catalytic and electrochemical properties. Platinum, though chemically inert and stable to high temperatures, has been known to react with alkali and alkaline-earth metals to form ternary platinum oxides. Several new ternary platinum oxide compounds were synthesized by the chemical attack on platinum crucible during work.

In a review by Schwartz and Prewitt, the structure and properties of binary and ternary oxides known at present can be seen in some detail (1). In the Ba–Pt–O system four phases were reported:  $\text{BaPtO}_3$  (2, 3),  $\text{Ba}_2\text{PtO}_4$ ,  $\text{Ba}_4\text{PtO}_6$  (4, 5), and there exists a solid solution series from 2:1 ( $\text{Ba}_2\text{PtO}_4$ ) to 1:1 ( $\text{BaPtO}_3$ ) that was first described by Schneider and McDaniel (4). This solid solution, with the general formula  $\text{Ba}_3\text{Pt}_{2+x}\text{O}_{7+2x}$ , was long identified by the formula  $\text{Ba}_3\text{Pt}_2\text{O}_7$  (6, 7). P. S. Haraden *et al.* (8) proposed a

structural model for  $\text{Ba}_3\text{Pt}_2\text{O}_7$ . Recently, anomalous diffraction and DAFS (diffraction anomalous fine structure) data on barium platinum oxide have been published (9, 10). A reinvestigation of this system has been undertaken, and it appears that the chemical formula of the solid solution corresponds in fact to the general formula  $\text{Ba}_{12}[\text{Ba}_x\text{Pt}_{3-x}]\text{Pt}_6\text{O}_{27}$  ( $0 \leq x \leq 3$ ) from  $\text{Ba}_{12}[\text{Pt}_3]\text{Pt}_6\text{O}_{27}$  ( $x = 0$ ) to  $\text{Ba}_{12}[\text{Ba}_3]\text{Pt}_6\text{O}_{27}$ . This solid solution corresponds to the  $n = 3$  member of the general family  $A_{3n+3}A'_nB_{n+3}O_{9+6n}$  (with  $A = \text{Ba}$ ,  $A' = \text{Ba/Pt}$ , and  $B = \text{Pt}$ ) proposed by Darriet *et al.* (11). This family is built up by the close stacking along the *c* direction of two kind of planes:  $[\text{A}_3\text{O}_9]$  and  $[\text{A}_3A'\text{O}_6]$ .

This paper is devoted to the synthesis, the crystallographic data obtained by electron microscopy, and the average crystal structure of a new compound  $\text{Ba}_{15}\text{Pt}_6\text{O}_{27}$  ( $x = 3$ ). We also report the results of electron diffraction characterization of  $\text{Ba}_{12}\text{Pt}_9\text{O}_{27}$  ( $x = 0$ ) as well as the evolution of the parameters of the solid solution when we varied  $x$  from 0 to 3. The structural relationships to the hexagonal perovskite, the  $\text{Sr}_4\text{PtO}_6$  type structure (12),  $\text{Sr}_4\text{Ni}_3\text{O}_9$  (13), and related compounds are discussed.

## EXPERIMENTAL

The synthesis of polycrystalline sample with the general formula  $\text{Ba}_{12}[\text{Ba}_x\text{Pt}_{3-x}]\text{Pt}_6\text{O}_{27}$  were initially prepared by firing the appropriate stoichiometric mixtures of  $\text{BaCO}_3$  (Aldrich 99.98%) and Pt metal (Aldrich 99.98%). The samples were mixed in an agate mortar and heated at 950°C for 24 h, 1050°C for 24 h, and a final heating step at 1150°C for 1 week with intermediate grinding and pelletizing. All the preparations were carried out under a flow of oxygen. Finally the powders were slowly cooled down to room temperature. The progress of the reaction was monitored using X-ray powder diffraction, and they were deemed to be complete when the diffraction pattern did not change on heating the sample further.

Powder X-ray diffraction data were recorded at room temperature on a Philips diffractometer using  $\text{CuK}\alpha$

radiation. Step scans were performed over the angular range  $5^\circ \leq 2\theta \leq 100^\circ$ , and a  $2\theta$  step size of  $0.02^\circ$  was used with an integration time of 10 s. Reitveld refinement (14) was performed using the FULLPROF program package (15). The peak shape was described by a pseudo-Voigt function, and the background level was defined by a polynomial function with six refinable coefficients. A scale factor, a counter-zero point, and the unit cell parameters were refined in addition to the atomic parameters.

Electron diffraction patterns were obtained with a JEOL 2000FX microscope, and the sample was prepared by crushing in alcohol.

## RESULTS AND DISCUSSION

### Characterization of $Ba_{12}Pt_9O_{27}$ ( $x = 0$ )

The X-ray diffraction pattern of this phase looks like the X-ray diffraction pattern of  $Ba_3Pt_2O_7$  (8) ( $a = 10.108 \text{ \AA}$  and  $c = 8.638 \text{ \AA}$ ). A tentative indexing has been undertaken: the best parameters found are  $a = 10.098(1) \text{ \AA}$  and  $c = 8.618(1) \text{ \AA}$ , but some reflections appear to shift from their theoretical positions. To clarify this point an electron diffraction study has been undertaken. Figure 1 presents a typical electron diffraction pattern for  $x = 0$ . It consists of an array of intense reflections which can be indexed on the basis of a hexagonal cell having  $a \approx 5.83 \text{ \AA} \approx a/\sqrt{3}$  and  $c \approx 4.31 \text{ \AA} \approx c/2$ . Around each intense reflection, up to four satellites are observed. The modulation appears to be incommensurate since the fourth-order satellites do not lie exactly along the  $[110]^*$  direction. So the whole pattern can be explained with a modulation vector  $q^* = \frac{1}{3}a^* + \frac{1}{3}b^* + 0.489c^*$  and an average trigonal lattice. Nevertheless, a careful examination of the intensity of the satellites shows that first-order satellites are often of higher intensity than the main spots: two subsystems exist with different periods along one direction. The crystal structure of  $Ba_{12}Pt_9O_{27}$  could be better described by considering a composite crystal rather than a modulated structure. So the electron diffraction pattern can be indexed with the following set of reciprocal vectors:  $a^*$ ,  $b^*$ ,  $c_1^*$ , and  $c_2^*$ , corresponding to  $a \approx 10.098 \text{ \AA}$ ,  $b_1 \approx 10.098 \text{ \AA}$ ,  $c_1 \approx 4.31 \text{ \AA}$ , and  $c_2 \approx 2.85 \text{ \AA}$ . Using this new basis, the reflection indexed as 1100 ( $hklm$ ) in Fig. 1 becomes 3000 ( $HKLm$ ). The first subsystem gives rise to  $HKL0$  reflections, and the second to  $HK0m$  reflections. In this pattern a systematic extinction occurs since the  $H0Lm$  reflections are observed only for  $L = 2n$ . The existence of this special reflection condition is confirmed in Fig. 2: in this pattern, all the  $HHL0$  reflections are observed. The  $(0, 0, 2n + 1, 0)$ , which should not be observed according to the previous condition appears in this pattern due to double diffraction. The very weak spots observed on this pattern are satellites as indicated by their indexation. Such a description using the concept of composite crystals has already been proposed to describe the structure of the related

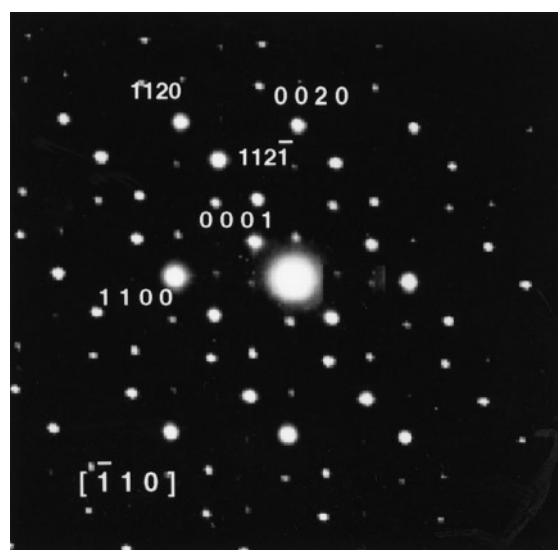


FIG. 1. Electron diffraction pattern of  $Ba_{12}Pt_9O_{27}$ , indexed with  $a = 5.83 \text{ \AA}$  and  $c = 4.31 \text{ \AA}$ , showing the modulation vector  $q^* = (\frac{1}{3}, \frac{1}{3}, 0.489)$ .

compound  $[Ba]_x[(Cu, Pt)O_3]$  ( $x = 1.317$ ) (16). In this composite crystal two mutually incommensurate subsystems are considered: the first subsystem is  $[Ba]$ , and the second is  $[(Cu, Pt)O_3]$ . This latter subsystem creates chains of face-sharing  $(Pt, Cu)O_6$  octahedra separated by a trigonal prism, between which are inserted barium columns (16). Using the structural model proposed by J. Darriet *et al.* (11), we can also describe this compound as the stacking of one close-packing  $[Ba_3O_9]$  layers, similar to those of the hexagonal perovskites, and three  $[BaA'O_6]$  layers ( $A' = Cu, Pt$ ).

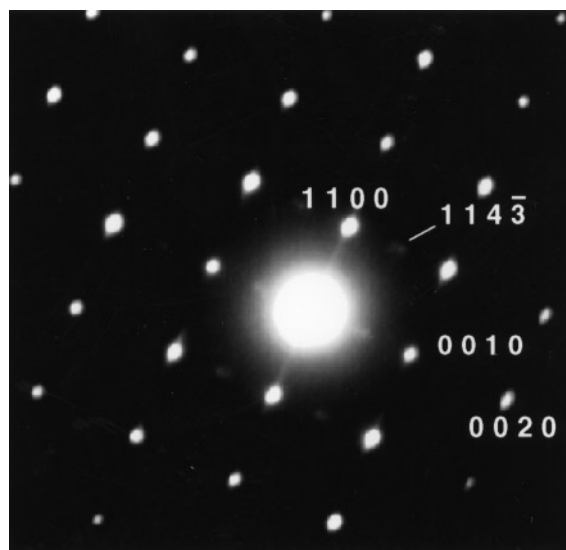


FIG. 2. Electron diffraction pattern of  $Ba_{12}Pt_9O_{27}$ , indexed in the conventional cell  $a^*$ ,  $b^*$ ,  $c_1^*$ , and  $c_2^*$ , showing the presence of the  $(0, 0, 2n + 1, 0)$  reflections.

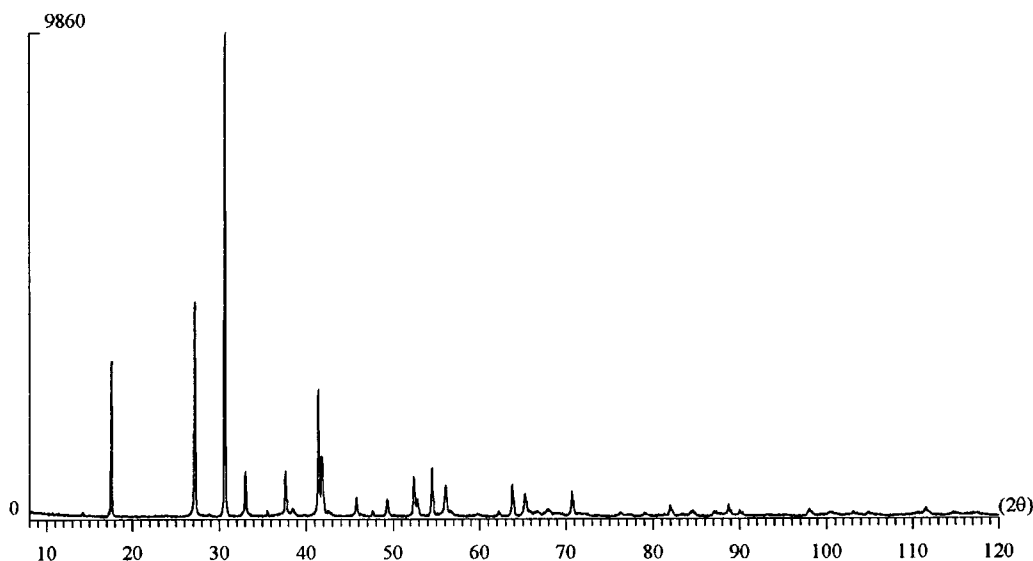


FIG. 3. Observed X-ray powder diffraction pattern of  $\text{Ba}_{12}\text{Pt}_9\text{O}_{27}$ .

The X-ray powder diffraction pattern (Fig. 3) has been indexed using a four-dimensional formalism as pointed out with the electron diffraction study. The corresponding indices are given in Table 1. The special reflection condition discussed above is verified by the indices. In addition, it clearly appears that the weakest peaks are assigned to the satellites, i.e. to indices with  $L$  and  $m$  not equal to 0. Both electron diffraction and X-ray diffraction indicate the presence of a centering condition:  $H - K - m = 3n$ .

#### Characterization of $\text{Ba}_{15}\text{Pt}_6\text{O}_{27}$ ( $x = 3$ )

The electron diffraction pattern obtained from this compound is shown in Fig. 4. All the reflections can be explained using the hexagonal cell determined by X-ray diffraction,  $a = 10.1560(5)$  Å and  $c = 8.830(5)$  Å. Nevertheless the distribution of the intensities of the reflections that appear on this pattern is rather similar to the distribution observed in Fig. 1. By analogy with our conclusion concerning  $\text{Ba}_{12}\text{Pt}_9\text{O}_{27}$ , this observation suggests  $\text{Ba}_{15}\text{Pt}_6\text{O}_{27}$  may be a commensurate modulated structure with parameters  $a = 5.867$  Å,  $c_1 = 4.415$  Å, and  $c_2 = 2.943$  Å.

The X-ray diffraction pattern can be indexed using the two descriptions (Table 2). At the first stage, a refinement of the structure, based on the known stacking sequence of the  $[\text{Ba}_3\text{O}_9]$  and  $[\text{Ba}_3(\text{Ba})\text{O}_6]$  planes, has been tried using the three-dimensional hexagonal cell. The atomic position of  $\text{Sr}_4\text{Ni}_3\text{O}_9$  as well as the space group ( $P321$ ) has been used as a trial model (13), since this compound is built up using the same stacking sequence of  $[\text{Sr}_3\text{O}_9]$  and  $[\text{Sr}_3\text{NiO}_6]$  layers as  $\text{Ba}_{15}\text{Pt}_6\text{O}_{27}$ . So barium atoms are placed in  $1a$  and  $2d$  positions (respectively Ni(4) and Ni(5) of Ref. (13)) which are

TABLE 1  
Indexation of the X-Ray Diffraction Pattern of  $\text{Ba}_{12}\text{Pt}_9\text{O}_{27}$

$d_{\text{obs}}$	$d_{\text{cal}}$	$HKLM$				$I/I_0$
6.208	6.207	1	0	-2	1	0.5
5.046	5.049	2	-1	0	0	41.0
3.278	3.278	1	1	1	0	45.4
3.091	3.095	1	2	2	-1	0.4
2.915	2.915	3	0	0	0	100.0
2.711	2.711	1	0	0	1	8.8
2.524	2.524	4	-2	0	0	1.0
2.388	2.389	0	2	0	1	9.5
2.337	2.338	3	1	2	-1	1.5
2.178	2.178	2	2	1	0	26.8
2.159	2.159	2	1	0	1	12.7
2.122	2.122	4	0	-2	1	1.2
1.980	1.982	2	-1	2	0	3.3
1.908	1.908	4	1	0	0	1.2
1.847	1.847	3	1	0	-1	3.7
1.745	1.745	4	1	1	0	8.0
1.731	1.733	3	0	2	0	3.7
1.683	1.683	6	-3	0	0	10.2
1.638	1.639	4	-2	2	0	6.1
1.623	1.624	4	2	2	-1	1
	1.622	6	-2	1	-1	
1.547	1.546	6	-1	-2	1	0.5
1.490	1.491	5	0	0	-1	0.8
1.458	1.457	6	0	0	0	6.7
1.428	1.428	4	1	2	0	4.8
		0	-1	6	-2	
1.399	1.400	1	3	1	1	0.9
		5	2	0	0	
1.379	1.380	5	1	-3	1	1.3
1.356	1.356	2	0	0	2	0.7

Note.  $a = 10.098$  Å,  $c_1 = 4.309$  Å,  $c_2 = 2.852$  Å. Reflection conditions:  $HKLM$ ,  $H - K - m = 3n$ ;  $HOLm$ ,  $L = 2n$ .

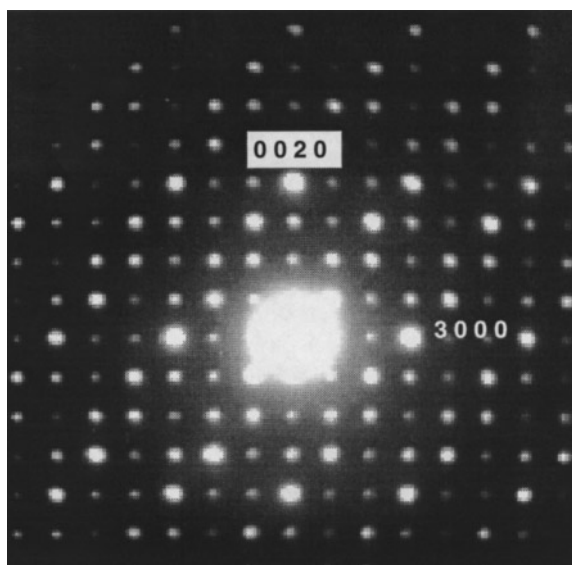


FIG. 4. Electron diffraction pattern of  $\text{Ba}_{15}\text{Pt}_6\text{O}_{27}$  indexed with  $a = 10.156 \text{ \AA}$ ,  $c_1 = 4.41 \text{ \AA}$ , and  $c_2 = 2.94 \text{ \AA}$ .

in the prismatic sites. Platinum atoms are located in  $2d$  and  $2c$  positions (respectively Ni(1), Ni(2), and Ni(3) of Ref. (13)). The temperature factors of oxygen atoms are fixed to realistic values. The obtained reliability factors are  $R_1 = 6.38\%$ ,  $R_p = 15.7\%$ , and  $R_{wp} = 19.3\%$ . The refined values are presented in Table 3, and the experimental, calculated, and difference patterns are shown in Fig. 5. The refinement reveals unlikely results. Even in fixing the temperature factor of oxygen, negative values of temperature factors (with no physical meaning) for platinum atoms (Pt3) and unusual interatomic distances (Table 4) are obtained, especially the mean  $\text{Ba}_4\text{-O}$  distance ( $d = 2.360 \text{ \AA}$ ), which is shorter than expected, and the  $\text{Pt}_2\text{-O}_3$  distance, which is too long ( $d = 2.310 \text{ \AA}$ ). These problems may indicate this phase is a commensurate modulated structure as already mentioned when we described the results of the electron diffraction experiment. The structure derived from the Rietveld refinement should then be considered as a basic structure. This structure is very similar to the structure of  $[\text{Ba}_x][(\text{Cu}, \text{Pt})\text{O}_3]$  ( $x = 1.317$ ) (16): it consists of columns of two face-sharing  $[\text{PtO}_6]$  octahedra followed by one face-sharing  $[\text{BaO}_6]$  trigonal prism (Fig. 6). The substitution of Pt atoms for barium atoms in the trigonal prism leads to the obtention of various composition with the general formula  $\text{Ba}_{12}[\text{Ba}_x\text{Pt}_{3-x}]\text{Pt}_6\text{O}_{27}$ .

#### Solid Solution $\text{Ba}_{12}[\text{Ba}_x\text{Pt}_{3-x}]\text{Pt}_6\text{O}_{27}$

We were able to prepare samples with the general formula  $\text{Ba}_{12}[\text{Ba}_x\text{Pt}_{3-x}]\text{Pt}_6\text{O}_{27}$  ( $x = 0, \frac{2}{3}, 1, \frac{4}{3}, 2, \frac{5}{2}, 3$ ). The pattern could be indexed using a hexagonal cell similar to that found for  $\text{Ba}_{15}\text{Pt}_6\text{O}_{27}$  ( $a = 10.1560 \text{ \AA}$ ,  $c = 8.830 \text{ \AA}$ ) for the

TABLE 2  
Indices of the X-Ray Diffraction Pattern of  $\text{Ba}_{15}\text{Pt}_6\text{O}_{27}$  ( $hkl$  Correspond to the Three-Dimensional Cell and  $HKLm$  to the Commensurate Modulated Cell)

$d_{\text{obs}}$	$d_{\text{cal}}$	$hkl$	$HKLm$				$I/I_0$
8.83	8.83	001	0	0	-2	1	1
6.23	6.23	101	1	0	1	-1	7
5.079	5.078	110	1	1	0	0	36
4.399	4.402	111	1	1	2	-1	1
	4.398	200	2	0	0	0	
3.938	3.936	201	2	0	2	-1	1
3.334	3.332	112	1	1	1	0	51
3.112	3.116	202	2	0	0	-2	2
	3.111	121	1	2	2	-1	
2.932	2.932	300	3	0	0	0	100
2.793	2.791	103	1	0	3	-1	11
2.539	2.539	220	2	2	0	0	4
2.447	2.446	023	0	2	0	1	1
	2.442	302	3	0	-1	0	
2.352	2.351	131	1	3	4	-3	6
2.201	2.204	123	1	2	0	1	44
	2.201	222	2	2	-1	0	
	2.199	400	4	0	0	0	
2.134	2.135	132	1	3	4	-2	3
	2.134	401	4	0	-1	1	
2.077	2.077	303	3	0	0	1	2
2.025	2.024	114	1	1	2	0	7
1.968	1.968	042	0	2	1	0	1
	1.967	321	3	2	-1	1	
1.919	1.923	223	2	2	0	-1	6
	1.919	410	4	1	0	0	
1.879	1.878	313	3	1	0	1	8
1.835	1.835	322	3	2	1	0	1
1.760	1.763	304	3	0	1	-2	13
	1.762	403	4	0	0	1	
	1.760	142	1	4	1	0	
	1.759	500	5	0	0	0	
1.725	1.725	501	5	0	-1	1	1
1.692	1.693	330	3	3	0	0	16
1.665	1.666	224	2	2	-2	0	14
	1.664	323	3	2	0	-1	
1.633	1.633	421	4	2	1	-1	2
	1.634	502	5	0	1	0	
1.608	1.608	413	4	1	0	-1	1
1.579	1.580	332	3	3	-1	0	1
		510	5	1	0	0	
1.555	1.558	404	4	0	0	0	2
	1.556	422	4	2	1	0	
		511	5	1	-2	1	
1.510	1.513	035	0	3	1	1	4
	1.51	503	5	0	-3	1	
1.466	1.467	333	3	3	0	-1	11
	1.466	060	0	6	0	0	
1.449	1.451	106	1	0	3	0	7
	1.450	225	2	2	-4	1	
	1.448	414	4	1	2	0	
	1.447	243	2	4	3	-1	
1.427	1.430	135	1	3	-1	-1	2
	1.427	431	4	3	2	-1	
1.414	1.413	116	1	1	0	2	3
1.408	1.408	520	5	2	0	0	3

TABLE 3  
Refined Crystallographic Data of  $\text{Ba}_{15}\text{Pt}_6\text{O}_{27}^a$

Atom	<i>x</i>	<i>y</i>	<i>z</i>	<i>B</i> (Å) <sup>2</sup>
Ba1	0.0219(8)	0.6856(7)	0.2588(5)	0.1(1)
Ba2	0.331(1)	0	0.5	1.6(2)
Ba3	0.3744(9)	0	0	1.0(2)
Ba4	0.6667	0.3333	0.243(1)	2.7(3)
Ba5	0	0	0	2.1(5)
Pt1	0.3333	0.6667	0.0967(9)	0.3(2)
Pt2	0.3333	0.6667	0.4168	1.9(2)
Pt3	0	0	0.3490(8)	−0.5(1)
O1	0.792(6)	0.475(6)	0.031(6)	0.5
O2	0.186(6)	0.031(6)	0.204(5)	0.5
O3	0.168(6)	0.501(6)	0.236(8)	0.5
O4	0.678(6)	0.193(5)	0.458(6)	0.5
O5	0.858(7)	0	0.5	0.5

<sup>a</sup>Space group, *P*321; *a* = 10.1560(5) Å, *c* = 8.8308(2) Å; *R*<sub>1</sub> = 5.84%; *R*<sub>p</sub> = 15.8%; *R*<sub>wp</sub> = 19.1%.

compounds with  $x \geq \frac{4}{3}$ . The X-ray diffraction pattern for the sample with  $0 \leq x \leq 1$  could not be indexed with such a cell but rather by using a cell similar to  $\text{Ba}_{12}\text{Pt}_9\text{O}_{27}$ . Figure 7a–c shows the variation of the *a*, *c*<sub>1</sub>, and *c*<sub>2</sub> parameters, respectively.

As it could be inferred from the structural model previously described (11), the *a* parameters do not vary with the *x* value, whereas the *c*<sub>1</sub> and *c*<sub>2</sub> parameters increase with increasing barium content. Nevertheless these latter

TABLE 4  
Selected Bond Lengths (Å) for  $\text{Ba}_{15}\text{Pt}_6\text{O}_{27}$

3 × Pt(1)–O(1)	2.084(5)	Ba(1)–O(1)	3.185(6)	2 × Ba(2)–O(2)	3.082(5)
3 × Pt(1)–O(3)	1.770(6)	Ba(1)–O(1)	3.015(6)	2 × Ba(2)–O(3)	2.891(7)
3 × Pt(2)–O(3)	2.320(7)	Ba(1)–O(2)	2.743(7)	2 × Ba(2)–O(4)	2.866(5)
3 × Pt(2)–O(4)	1.850(7)	Ba(1)–O(2)	3.069(6)	2 × Ba(2)–O(2)	3.077(7)
3 × Pt(3)–O(2)	2.174(6)	Ba(1)–O(3)	2.926(7)	2 × Ba(2)–O(5)	2.922(7)
3 × Pt(3)–O(5)	1.964(2)	Ba(1)–O(3)	2.740(7)	3 × Ba(4)–O(4)	2.404(6)
Pt(3)–Pt(3)	2.666(1)	Ba(1)–O(4)	2.753(6)	3 × Ba(4)–O(1)	2.323(6)
2 × Ba(3)–O(1)	2.796(5)	Ba(1)–O(4)	3.071(6)	6 × Ba(5)–O(2)	2.525(7)
2 × Ba(3)–O(1)	2.785(6)	Ba(1)–O(5)	2.834(3)		
2 × Ba(3)–O(2)	2.754(6)	2 × Ba(3)–O(3)	2.595(7)		

parameters do not obey the same variation rule. The *c*<sub>2</sub> parameter, which corresponds to the [(Ba, Pt)O<sub>3</sub>] subsystem, continuously increases with *x* as expected, whereas a discontinuity is observed in the variation of *c*<sub>1</sub> around  $x \approx 1$ . This point corresponds to the transition incommensurate–commensurate modulated structure observed by X-ray diffraction. As *c*<sub>1</sub> is related to the [Ba] subsystem we may think that the incommensurate modulation could be due to the large radius of the Ba atoms which cannot follow the shrinkage of the average interlayer distance ( $d = 2.208$  Å for  $\text{Ba}_{15}\text{Pt}_6\text{O}_{27}$  and  $d = 2.154$  Å for  $\text{Ba}_{12}\text{Pt}_9\text{O}_{27}$ ) due to the progressive substitution of Pt atoms for Ba atoms. This hypothesis must be confirmed by a complete determination of the structure of these phases, using the 4D crystallography.

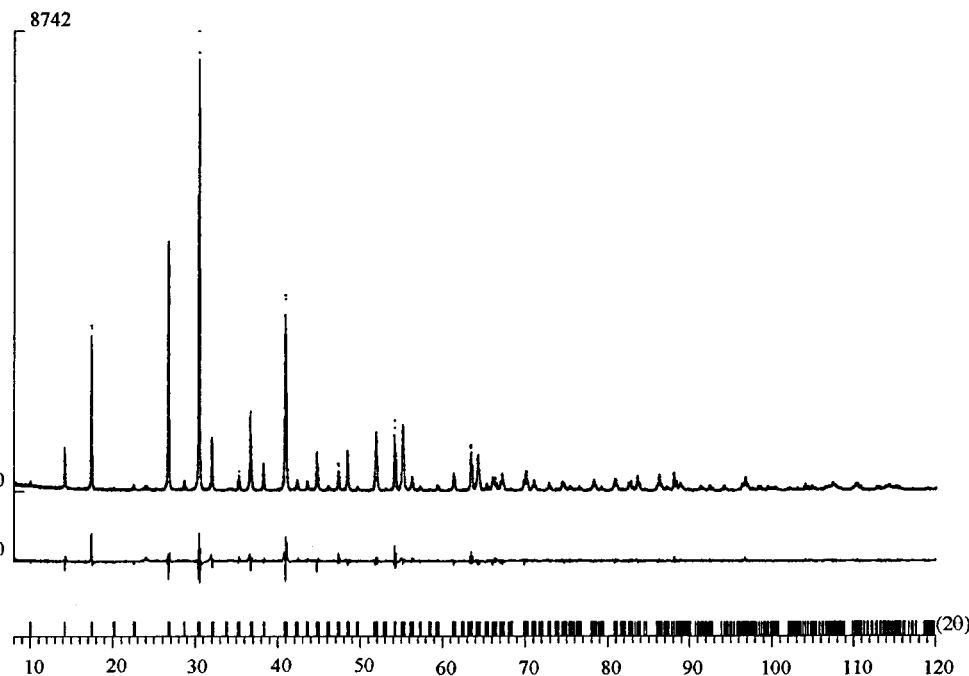


FIG. 5. Observed (dots), calculated (full line), and difference X-ray powder diffraction profiles of  $\text{Ba}_{15}\text{Pt}_6\text{O}_{27}$ .

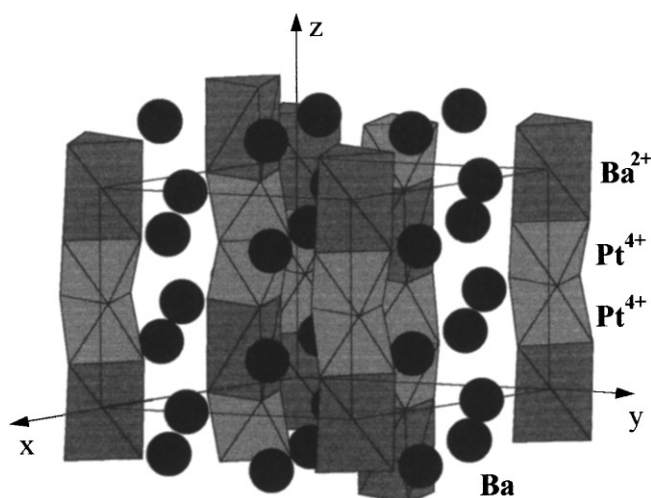


FIG. 6. Representation of the basic structure of  $\text{Ba}_{15}\text{Pt}_6\text{O}_{27}$ .

### CONCLUSION

The barium-rich region of Ba-Pt-O system has been reinvestigated. We point out the existence of a solid solu-

tion corresponding to the general chemical formula  $\text{Ba}_{12}[\text{Ba}_x\text{Pt}_{3-x}]\text{Pt}_6\text{O}_{27}$ . The evolution of the parameters has been measured. A tentative crystallographic determination has been undertaken of the two extreme compounds.  $\text{Ba}_{12}\text{Pt}_9\text{O}_{27}$  appears to be a composite crystal with two subsystems: [Ba] and [PtO<sub>3</sub>]. A similar description may be adopted for  $\text{Ba}_{15}\text{Pt}_6\text{O}_{27}$ , even if this phase appears to be a commensurate modulated structure.

These phases are the  $n = 3$  member of the general family  $A_{3n+3}A'_nB_{3+n}O_{9+6n}$  already described (11). It can be compared with  $\text{Sr}_4\text{Ru}_2\text{O}_9$  (17) ( $n = 3$ ),  $\text{Sr}_4\text{Ni}_3\text{O}_9$  (13) ( $n = 3$ ), and  $\text{Ba}_4\text{PtO}_6$  ( $n = \infty$ ) (5). In all these phases, prismatic sites can be found which are either empty (17) or occupied by transition metals (13) or alkaline-earth metals (5). The basic structure we present for  $\text{Ba}_{15}\text{Pt}_6\text{O}_{27}$  shows that the prismatic sites are occupied by  $\text{Ba}^{2+}$  cations as in  $\text{Ba}_4\text{PtO}_6$ . The extrapolation to  $\text{Ba}_{12}\text{Pt}_9\text{O}_{27}$  indicates that in this latter compound the prismatic sites should be occupied by  $\text{Pt}^{2+}$  cations. The complete structural determination using the (3+1) crystallography is now in progress on a single crystal.

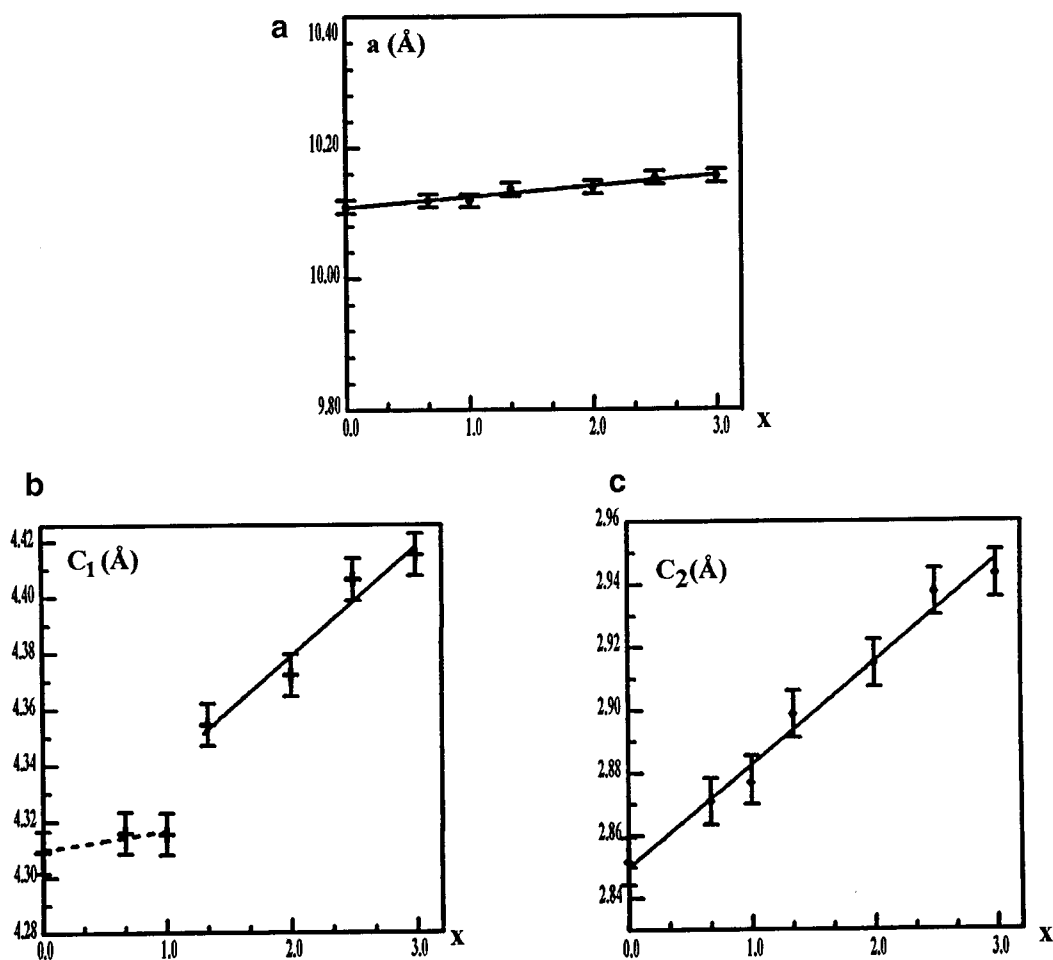


FIG. 7. Representation of the variation of  $a$  (a),  $c_1$  (b), and  $c_2$  (c) parameters of  $\text{Ba}_{12}[\text{Ba}_x\text{Pt}_{3-x}]\text{Pt}_6\text{O}_{27}$  ( $0 \leq x \leq 3$ ).

## REFERENCES

1. K. B. Schwartz and C. T. Prewitt, *J. Phys. Chem. Solid* **45**(1), 1 (1984).
2. P. K. Gallagher, D. W. Johnson, Jr., E. M. Vogel, G. K. Wertheim, and F. J. Schnetter, *J. Solid State Chem.* **21**, 277 (1977).
3. B. L. Chamberland and S. Silverman, *J. Less Common Metals* **65**, 41 (1979).
4. S. J. Schneider and C. L. McDaniel, *J. Am. Ceram. Soc.* **52**, 518 (1969).
5. A. P. Wilkinson and A. K. Cheetham, *Acta Crystallogr.* **C45**, 1672 (1989).
6. G. Rousseau, *C. R. Acad. Sci. Paris* **109**, 144 (1889).
7. W. O. Statton, *J. Chem. Phys.* **19**, 3 (1951).
8. P. S. Haraden, L. Chamberland, L. Katz, and A. Gleyzes, *J. Solid State Chem.* **21**, 217 (1977).
9. J. Vacinova, J. L. Hodeau, P. Wolfers, E. Alkaim, J. P. Lauriat, B. Bouchet-Fabre, and B. L. Chamberland, *Nucl. Instr. Methods Phys. Res.* **B97**, 102 (1995).
10. J. Vacinova, J. L. Hodeau, P. Wolfers, J. P. Lauriat, and E. Alkaim, *J. Synchrotron Rad.* **2**, 236 (1995).
11. J. Darriet and M. A. Subramanian, *J. Mater. Chem.* **5**(4), 543 (1995).
12. J. J. Randall and L. Katz, *Acta Crystallogr.* **12**, 519 (1959).
13. F. Abraham, S. Minaud, and C. Renard, *J. Mater. Chem.* **4**(11), 1763 (1994).
14. H. M. Rietveld, *J. Appl. Crystallogr.* **2**, 65 (1969).
15. J. Rodriguez-Carvajal, FULLPROF. LLB.CE, Saclay, France, 1997.
16. K. Ukey, A. Yamamoto, Y. Watanabe, T. Shishido, and T. Fukuda, *Acta Crystallogr.* **B49**, 67 (1963).
17. C. Dussarrat, J. Fompeyrine, and J. Darriet, *Eur. J. Solid State Inorg. Chem.* **32**, 3 (1995).